The Effect of Tip Clearance on the Performance of an Axial Flow Fan

FRANCIS J. RYAN
HIROSHI OHASHI

REPORT NO. 31

GAS TURBINE LABORATORY
MASSACHUSETTS INSTITUTE OF TECHNOLOGY
CAMBRIDGE · 39 · MASSACHUSETTS

THREE-DIMENSIONAL FLOW IN TURBOMACHINE RESEARCH

THE EFFECT OF TIP CLEARANCE ON AN AXIAL FLOW FAN

Francis J. Ryan
Hiroshi Ohashi

Under the sponsorship of:

General Electric Company
Westinghouse Electric Corporation
Curtiss-Wright Corporation
Allison Division of the General Motors Corporation

Gas Turbine Laboratory
Report Number 31
May 1955

Massachusetts Institute of Technology

ABSTRACT

The effect of tip clearance on the performance of a single stage axial flow (6000 cfm) fan was investigated for tip clearances ranging from 0.003 in. to 0.252 in. It was found that, at the rated flow, the stagnation pressure rise (mass flow weighted) across the fan rotor was a maximum for the smallest tip clearance and a minimum for the largest tip clearance. However, it was found also that at the rated flow, the stagnation pressure rise was larger at a tip clearance of 0.022 in. than at a tip clearance of 0.015 in. At a flow of 4000 cfm (two-thirds of rated flow) the effect of tip clearance was found to be negligible over the entire range of clearances tested. At flows in excess of 6500 cfm, the stagnation pressure rise was highest for a tip clearance of 0.022 in.

Plotting a performance map of stagnation pressure rise across the rotor versus volume flow also revealed that as the peak pressures became higher, these peaks shifted to lower values of flow. This would indicate a shifting of the surge line vertically and horizontally on the performance map as the tip clearance is varied.

The flow pattern in the original fan, as manufactured, was investigated also. This revealed that, at the rated flow, the suction sides of the stator blades were stalled over approximately the after one-half of their surface while the pressure sides were completely unstalled. This study also showed that, at all flows tested, the flow pattern at the rotor tip was somewhat turbulent, while the pattern at the rotor root was stable at high flows but became very unstable at low flows. At flows below 5000 cfm reversal of flow started near the rotor tip.

ACKNOWLEDGMENTS

This investigation was carried out by the authors in the M.I.T. Gas Turbine Laboratory under the supervision of Professor Robert C. Dean, Jr. The substance of this report is contained in the authors' thesis for the degree of Master of Science, Mechanical Engineering Department, M.I.T., 1955.

The research was sponsored by the General Electric Company, the Westinghouse Electric Corporation, the Curtiss-Wright Corporation and the Allison Division of the General Motors Corporation.

The authors wish to express their sincere thanks to Professor Dean for his generous help and many suggestions; to Mr. Dalton Baugh and Mr. Simon Beisheim for their help in constructing the test apparatus; and to Miss Barbara Shuster and Mrs. David V. Stallard for help in preparing the manuscript.

TABLE OF CONTENTS

INDEX OF FIGURES

NOMENCLATURE

A	Area
c	Chord
C	Velocity
H	Shape factor
p	Pressure
Q	Volume flow
r	Radius
s	Pitch
U	Linear rotor tip velocity
W	Shaft work per pound of fluid
B.L.	Boundary layer
T.C.	Tip clearance
β	Blade angle
δ	Thickness of boundary layer ($.98 \frac{C}{C_{M.S.}}$)
δ^*	Displacement thickness of boundary layer
η	Efficiency $(\Delta p_o/\rho)/W$
ω	Angular velocity
ρ	Density
θ	Momentum thickness of boundary layer
ζ	Stagger angle

Subscripts

o	Stagnation value
s	Static value
x	Axial direction
i	Local value
M.S.	Mainstream

Superscripts

-	Mass flow weighted

1. Introduction

An investigation of the effect of tip clearance on the performance of a single stage axial fan has been made by Ruden, (Reference 1). In this study he varied the tip clearance to rotor diameter ratio from 0.002 to 0.012 and found that the fan efficiency decreased with increasing tip clearance over the entire range of throttling coefficients he used. The original diameter of the rotor was 500 mm. which indicates that his smallest tip clearance was 1 mm. (0.039 in.) and his largest tip clearance was 6mm. (0.234 in.). He concludes that extrapolation by a straight line from the minimum test clearance back to zero clearance may be made thus, giving steadily higher efficiencies as the tip clearance is reduced.

The effect of tip clearance on a cascade with stationary or moving end wall has been investigated by Dean, et al (Reference 2). In these cascade tests the tip clearance was varied from zero to 0.28 in. for the stationary wall and from 0.095 in. to 0.28 in. for the moving wall. For the stationary wall cascade, over the range tested, losses were shown to be a minimum at zero tip clearance, to increase to a relative maximum at 0.095 in. tip clearance, to decrease considerably at a tip clearance of approximately 0.145 in., and then to rise steadily at still larger clearances. For the moving wall cascade, losses were shown as maximum at the largest tip clearance and as minimum near the region of the smallest tip clearance, but too few data points were available at small clearances to define the curve clearly.

After the cascade tests it was felt that it would be of considerable interest to re-examine the effect of tip clearance on the performance of a single stage axial flow fan especially in the region below that of Ruden's tests. The primary purpose was to determine if a basis of comparison exists between tip clearance effects in cascade and in actual turbomachinery.

Stagnation pressure rise across the rotor was measured for six tip clearance values at flows from 3200 cfm to 7500 cfm. A performance map was plotted. The velocity profiles before the rotor were measured. The flow pattern in the fan was studied by means of hot-wire anemometer equipment, carbon-black tests, and tufts inserted at various points in the air stream.

Since the rotor blades on the fan were tapered and thus of changing cross section with radius, and since the tip clearance on the original fan varied widely around the circumference, it was decided not to vary the tip clearance by progressively machining down the blades. Rather a type of casing was used which could be progressively enlarged by a boring method designed to insure accurate dimensions and good concentricity. This procedure kept constant the rotor diameter and, thus, the rotor tip velocity. The special casing and the method of varying the tip clearance are described under Apparatus.

Since preliminary smoke tests showed flow reversal near the rotor tip at low flows, a study was undertaken of flow pattern in the original fan before tip clearances were altered. Those results are reported herein.

2. Description of Test Apparatus

2.1 The Test Fan

The fan is a single stage axial flow 6000 cfm fan manufactured by the Sturtevant Division of the Westinghouse Corporation. The rotor contains seven blades, pertinent blade data is as follows:

	Tip	Mean	Root
Radius, r, (in.)	12.5	10.7	8.2
Chord, c, (in.)	6.0	7.4	9.1
Pitch, s, (in.)	11.2	9.6	7.4
Stagger angle, ξ, (degrees)	69.0	62.5	49.0
Blade inlet angle, β_1, (degrees)	74.0	70.5	63.5
Blade outlet angle, β_2, (degrees)	64.0	55.5	37.5
Wheel speed, ωr, (ft./sec.)	193	165	127

The rotor blade sections were modified NACA 4-digit series profiles.

The fan housing contains ten stator blades, 4 5/16 in. in height with a chord length of 11 in. The motor is a 440 volt, 60 cps, three phase induction type with two speeds (1150 rpm and 1735 rpm). Only the high speed, 1735 rpm, was used in these tests.

The discharge ducting and straightening tubes are shown in Figure 2. The bell-mouth is a 27 in. diameter rubber inner tube inflated to the desired size.

The special casing, was formed of heavy perforated sheet metal covered inside with a thick layer of a special pattern-molding type of plaster. This casing was bored out to desired size by means of a boring tool mounted on the rotor shaft itself thus insuring good concentricity.

2.2 Flow Measurement Equipment

The flow was controlled by means of a throttle located five feet downstream from the metering station. This flow metering station is located two feet downstream from the straightening tubes and consists of a combined pitot tube connected to an inclined manometer.

2.3 Pressure Measuring Equipment

A Kiel probe rake was located just aft of the trailing edge of the rotor blades. This rake consists of six tubes arranged radially as shown in Figure 3. A stagnation pressure rake containing six tubes was located downstream from the stator blades; it is described in Figure 3.

Four static pressure taps behind the rotor were located as follows: two on the wall of the outer casing and two on the inner casing straddling the Kiel rake position. All the above pressure measuring devices were connected to a fourteen tube water manometer.

2.4 Flow Angle Measurement

To measure the angle at which the flow leaves the rotor blades, a lucite window was installed in the casing behind the rotor. A tuft of wool fiber was attached to the end of a slender rod in such a manner that the tuft was free to rotate. This rod was inserted through a small hole in the lucite window; a protractor was mounted on the surface of the window. The tuft could be traversed radially and the angle between the tuft and the axial direction could be measured at any radial station.

2.5 Boundary Layer Measurement

For the inlet boundary measurements, a traversing Kiel probe was located four inches upstream from the rotor together with a wall static pressure tap beside the Kiel probe. These taps were connected to an inclined manometer.

2.6 The Hot-Wire Anemometer Apparatus

The hot-wire anemometer probe was located immediately after the trailing edge of the rotor blade. The signal was fed through an amplifier and thence to a cathode ray oscilloscope. A signal of known frequency, corresponding to the blade-wake frequency, was generated by an oscillator and superimposed on the z-axis of the oscilloscope in order to distinguish the blade-wakes from stall cells or other flow discontinuities.

3. Tests and Data

In this investigation the tip clearances tested were as follows: 0.003, 0.015, 0.022, 0.062, 0.153, and 0.252 in. At each of these clearances, the flow was varied in seven steps from 3200 cfm to 7500 cfm; a set of stagnation pressure, static pressure and flow angle readings behind the rotor were taken at each step. A linear distribution of static pressure from inner to outer casing was assumed. The stagnation pressure rise (mass-flow weighted as described in the Appendix) across the rotor was then plotted versus volume flow for each of the tip clearances in Figure 4.

Flow calibration and boundary layer measurements were accomplished as described in the Appendix. The flow pattern in the original fan as manufactured was studied by means of carbon-black tests, hot-wire anemometer traverses and tufts inserted in the air stream.

4. Results

4.1 Fan Performance

Inspection of Figures 4 and 5 reveals:

1. At the rated flow (6000 cfm), the maximum stagnation pressure rise (mass-flow weighted) across the rotor occurred at the minimum tip clearance (0.003 in.) tested while the minimum pressure rise occurred at the largest tip clearance (0.252 in.) tested. It seems of particular interest, however, to note that, at this same rated flow, the pressure rise was greater at a tip clearance of 0.022 in. than at a tip clearance of 0.015 in.

2. At a flow of 4000 cfm (two-thirds rated flow) the pressure rise across the rotor was independent, approximately, of the value of tip clearance.

3. At flows in excess of approximately 6500 cfm, the pressure rise was highest for a tip clearance of 0.022 in. even though two smaller clearances also were tested.

4. As the peak pressure rise across the rotor increased,there was a lateral shifting of these peaks to lower values of flow. This indicates a shifting of the surge line horizontally and vertically.

5. In the region of the rated flow (6000 cfm) the performance curve provided by the fan manufacturer falls between the measured curves for tip clearances of 0.062 in. and 0.153 in. Since the maximum allowable clearance on the working drawings is approximately 0.076 in. and since the performance curve probably corresponds to a fan with maximum clearance (i.e. minimum acceptable performance), it would be predicted from the results of the present tests that the manufacturer's curve should lie where it does at rated flow. This correspondence provides, at least, a partial check on the data collected in this investigation.

4.2 Flow Pattern

1. The velocity profiles in Figure 6 indicate an inlet boundary layer thickness, δ, of approximately one-half inch; this value is the one used for the calculation of tip clearance to boundary layer thickness appearing later in this report. The graph shown is for a tip clearance of 0.022 in. but runs taken at other tip clearances showed little change.

2. The flow pattern at inlet to the original fan is indicated by the photograph of tufts which appears in Figure 8. These tufts were inserted upstream of the rotor and show that the flow was axially inward over the entire inlet diameter at high flows and then gradually entered less and less axially as the flow was reduced until, at very low flows, the flow reversed in some regions of the inlet diameter.

3. Study of the flow pattern in the stator passages of the original fan, by means of carbon-black and oil spread on the suction and pressure sides of the stator blades, revealed, that, at the rated flow, the suction side of the blades was stalled over approximately the after one-half of its surface while the pressure side was completely unstalled. This is shown schematically in Figure 10-a.

4. The photographs of the oscilloscope screen appearing in Figure 9 indicate that at high flows, the pattern behind the rotor shows well-defined traces of the blade wakes at the root with but very little distrubance between wakes. At the tip, the blade wakes are not defined so clearly and more turbulence is evident. At low flows, however, the pattern shows large turbulence at the root while the pattern at the tip stays approximately the same as at high flows. The set of photographs in Figure 9 were taken at a tip clearance of 0.022 in.; similar photographs taken at other tip clearances showed much the same sequence. The line of dots appearing in each photograph is a frequency of 205 cps superimposed on the z-axis of the oscilloscope and corresponds approximately to the blade-passing frequency.

5. An estimation of the flow pattern through the fan, based on the study of the carbon-black tests, the hot-wire anemometer traverses, and the observations of the tufts in the airstream at various points appears in Figures 10-a and 10-b.

5. Discussion and Conclusions

5.1 Performance Map Significances

The main significance of the performance map seems to be the indication that within the range of practical tip clearances there may be an optimum value for best performance and this optimum clearance may not be the minimum. Alteration of the position of the surge point with variation in tip clearance is of significance also.

5.2 Comparison with the Cascade Data of Reference 2.

In order to compare the results of the present tests with the cascade tests as reported by Dean, it may be of interest to non-dimensionalize the tip clearances used in the present tests into percentages of tip chord length, boundary layer thickness, and displacement thickness for the boundary layer as follows:

T.C.	T.C./c(%)	T.C./δ(%)	T.C./δ^*(%)
0.003	0.05	0.60	4.41
0.015	0.25	3.00	22.05
0.022	0.37	4.44	32.63
0.062	1.03	12.36	90.85
0.153	2.55	30.60	224.91
0.252	4.20	50.40	370.44

In the stationary wall cascade, a relative minimum loss point was observed at a T.C./c ratio of approximately 5.2% which corresponds to a T.C./δ^* of 104%. While sufficient data at small clearances is not available for the moving wall cascade, the boundary layer data of Reference 2 might lead one to expect minimum loss for the moving wall cascade at a T.C./c of 4% or a T.C./δ^* of 80%. By comparing these cascade results with the table above, it is evident that these clearances for minimum loss do not show close agreement with the maximum stagnation pressure rise points in the present tests. However, both the cascade tests and the present tests do show a similar trend of loss and stagnation pressure rise, respectively, with increasing tip clearance.

The cascade results show that the tangential force exerted on the fluid by the blades is independent, approximately, of tip clearance up to a value of 10% of the blade chord. If, in addition, it is assumed that the mass flow through the rotor tip region is not altered significantly by small tip clearances (less than 0.050 in.) then the work per pound of fluid should be constant. The stagnation pressure rise is given by:

$$\frac{\Delta p_o}{\rho} = \eta \frac{\text{work}}{\text{lbm}}$$

With the constant work assumption, it would appear that, since the stagnation pressure rise, Δp_o, varies with tip clearance, then the efficiency, η, must be a function of tip clearance. The increase in stagnation pressure rise with increasing tip clearance evident in Figure 5 would be explained, then, by an increase in efficiency with increasing tip clearance.

One source of numerical discrepancy, when comparing the results of the present tests with the cascade tests, might be the fact that the value of C_x/U was infinite for the stationary wall cascade and 0.64 for the moving wall cascade while for the present tests the value was 0.22.

5.3 Consideration of Leakage Loss

It may be of interest to compare the magnitude of the stagnation pressure loss due to tip clearance leakage and subsequent downstream mixing as computed from an idealized model with the measured changes in stagnation pressure rise. In this model, it is assumed that only the air passing through the rotor has work done on it, but the air leaking through the clearance space is assumed to be subject to no work from the rotor. The "worked" and "unworked" air is then assumed to mix at constant area downstream of the rotor to a uniform velocity. As shown in the Appendix, we obtain for this model the expression:

$$(\Delta P_o)_{T.C.\neq 0} = (\Delta P_o)_{T.C.=0} \left[\frac{1}{1 + \frac{A_{T.C.}}{A_{ROTOR}} \sqrt{1 + \frac{2g_o}{\rho Q^2} (A_{T.C.} + A_{ROTOR})^2 (\Delta P_o)_{T.C.=0}}} \right]$$

where $A_{T.C.}$ = leakage area

A_{rotor} = annulus area of rotor

$(\Delta P_o)_{T.C.=0}$ = stagnation pressure rise across rotor for zero tip clearance.

$(\Delta P_o)_{T.C.\neq 0}$ = stagnation pressure rise across rotor for a given tip clearance.

Q = total flow rate

The stagnation pressure rise computed from this expression is plotted on Figure 5; it does not explain the measured values. In particular, it does not explain the increase in stagnation pressure rise between tip clearances of 0.015 in. and 0.022 in. Neither does the model explain the small variation in stagnation pressure rise with increasing tip clearance at 4000 cfm.

5.4 Flow Pattern

Since, as indicated in Figures 10 (a) and 10 (b), the flow near the rotor tip shows evidence of significant radial components at through flows somewhat below 5000 cfm, it would appear that tip separation is severe below this flow rate. Some of the effects of tip clearance, as evidenced in Figures 4 and 5, may be attributed to this separation of the flow from the blades. When the tip is unstalled at large through flows, tip clearance effects should be, and were observed to be, significant. However, when the rotor tip is stalled thoroughly, tip leakage should have little effect for the range of clearances tested. This conclusion can explain the small effect of tip clearance at a flow of 4000 cfm.

APPENDIX

A.1 Test Procedure and Reduction of Data

A.1.1 Flow Calibration

The readings of stagnation pressure and static pressure were taken at the metering station by means of the pitot tube arrangement discussed under Apparatus for various settings of the throttling device. The pitot tube was traversed radially in both the horizontal and vertical planes. Pressure readings were taken at the following radial stations: 6.57", 4.33", 2.81", 1.56", 0.38" from the inner surface of the pipe. The velocity at each radial station was computed by:

$$p_o - p_s = \frac{\rho}{2g_o} C^2$$

The square root of each of these local velocities was summed and divided by the number of stations, then squared and this value was taken as the mean velocity in the cross section.

The volume flow was then computed by:

$$Q = AC_{mean}$$

This procedure was repeated for various throttle settings.

It was found that the velocity at the radial station 4.33" from the surface in the vertical direction closely approximated the mean velocity as computed above. The pitot tube was set, therefore, at this radial station. A plot of volume flow versus pitot tube reading for all subsequent runs appears as Figure 7.

A.1.2 Stagnation Pressure Rise Across the Rotor

At each tip clearance, the flow was varied in seven steps from approximately 3200 cfm to 7500 cfm. A set of stagnation and static pressure readings were taken from the probes located just downstream from the rotor. Simultaneous readings of the flow angle leaving the rotor at each radius were taken by means of the tuft and protractor device described under Apparatus.

The static pressures on the inside casing and outside casing were plotted and a linear variation was assumed from inner to outer wall to give a static pressure distribution behind the rotor.

The stagnation pressures were taken from the Kiel probe rake at the six radial stations described under Apparatus. Knowing both the stagnation and static pressures at each of these stations the local velocities were computed by:

$$(p_o - p_s)_i = \frac{\rho}{2g_o} C_i^2$$

From angle measurements, the axial components of each of these local velocities were computed. The area at each of the six radial stations was taken as the annular area of which the station is approximately the mean. The volume flow through each of these annular areas was then computed, knowing the area and the axial velocity component, by:

$$Q_i = A_i C_{xi}$$

The mass flow weighted stagnation pressure rise across the rotor was computed by:

$$\overline{\Delta P_o} = \frac{\sum_{i=1}^{6} Q_i \Delta P_{oi}}{\sum_{i=1}^{6} Q_i}$$

This weighted stagnation pressure is plotted versus volume flow for each tip clearance in Figure 4.

A.1.3 Boundary Layer Measurement

At a point four inches upstream of the rotor a measuring station consisting of a traversing Kiel probe and a near-by wall static tap was installed. For a tip clearance of 0.022 in. and for flows of 5000, 6000, 7000 and 7700 cfm, readings of the difference between stagnation pressure as picked up by the Kiel probe and static pressure as picked up by the wall tap were made as the Kiel probe was traversed radially. The diameter of the Kiel probe shroud is 5/32 in., therefore, the radial traverse station nearest the wall is 5/64 in. from the surface.

A.1.4 Calculation of Boundary Layer Parameters (before rotor)

A. Displacement thickness

$$\delta^* = \int_0^{\delta} \left(1 - \frac{C}{C_{M.S.}}\right) dZ$$

= 0.068 for rated flow

B. Momentum thickness

$$\theta = \int_0^{\delta} \frac{C}{C_{M.S.}} \left(1 - \frac{C}{C_{M.S.}}\right) dZ$$

= 0.051 for rated flow

C. Shape factor

$$H = \frac{\delta^*}{\theta}$$

= 1.33 for rated flow

A.2 Idealized Model

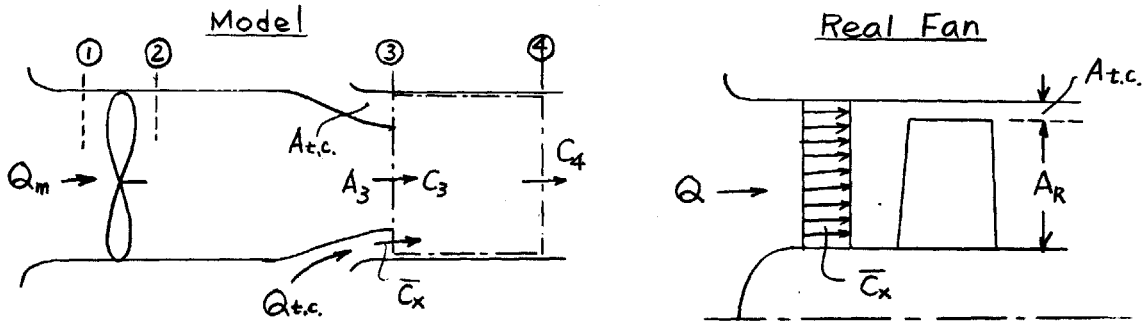

Regard T.C. = .003" as zero tip clearance

$$(\Delta p_o)_{1-2} = (\Delta p_o)_{t.c.=0} = (\Delta p_o)_{t.c.=0.003"}$$

Assumptions: (1) isentropic acceleration between (2) and (3)

(2) constant area mixing without friction between (3) and (4)

(3) the axial velocity of flow through the leakage area annulus of the real fan is equal to the bulk mean axial velocity of the actual flow, $\bar{C}_x$

Definition of Stagnation Pressure

$$P_{o2} = P_a + (\Delta P_o)_{t.c.=0} \qquad \text{.....(1)}$$

$$P_{o2} = P_3 + \frac{\rho C_3^2}{2 g_o} \qquad \text{.....(2)}$$

Bernoulli's equation along a streamline of the leakage flow, $Q_{t.c.} = 0$

$$P_a = P_3 + \frac{\rho \bar{C}_x^2}{2 g_o} \qquad \text{.....(3)}$$

Momentum equation for mixing

$$(P_3 - P_4)(A_3 + A_{t.c.}) = \frac{1}{2g_0}\left[\rho C_4^2 (A_3 + A_{t.c.}) - \rho\{C_3^2 A_3 + \overline{C_x}^2 A_{t.c.}\}\right] \qquad \ldots\ldots\ldots(4)$$

Continuity

$$A_3 C_3 = A_R \overline{C_x} = Q_m \qquad \ldots\ldots\ldots(5)$$

Eliminate P_3, P_4, C_3, C_4, and A_3, noting $Q = Q_m + Q_{t.c.}$

$$(\Delta P_0)_{t.c.\neq 0} = \frac{(\Delta P_0)_{t.c.=0}}{1 + \frac{A_{t.c.}}{A_R}\sqrt{1 + \frac{2g_0}{\rho Q^2}(A_{t.c.} + A_R)^2 (\Delta P_0)_{t.c.=0}}}$$

BIBLIOGRAPHY

1. Ruden, P., "Investigation of Single Stage Axial Fans", NACA TM 1062, 1944.

2. Dean, R.C., Jr., "The Influence of Tip Clearance on Boundary-Layer Flow in a Rectilinear Cascade", Report No. 27-3, Gas Turbine Laboratory, M.I.T., 1954.

3. Weske, J.R., "An Investigation of the Aerodynamic Characteristics of a Rotating Axial-Flow Blade Grid", NACA TN 1128, 1947.

4. National Association of Fan Manufacturers, Inc., "Standard Definitions, Terms and Test Codes for Centrifugal, Axial and Propeller Fans", Bulletin No. 110, 1952.

5. Dean, R.C., Jr., "Aerodynamic Measurements", Gas Turbine Laboratory, M.I.T., 1953.

6. Shapiro, A.H., "The Dynamics and Thermodynamics of Compressible Fluid Flow", The Ronald Press Company, New York, 1953.

7. American Society of Mechanical Engineers, "Test Code for Fans", 1946.

8. Kline, S.J. and McClintock, F.A., "Describing Uncertainties in Single Sample Experiments", Mechanical Engineering, January 1953.

9. Keller, C., "The Theory and Performance of Axial-Flow Fans", McGraw-Hill, 1937.

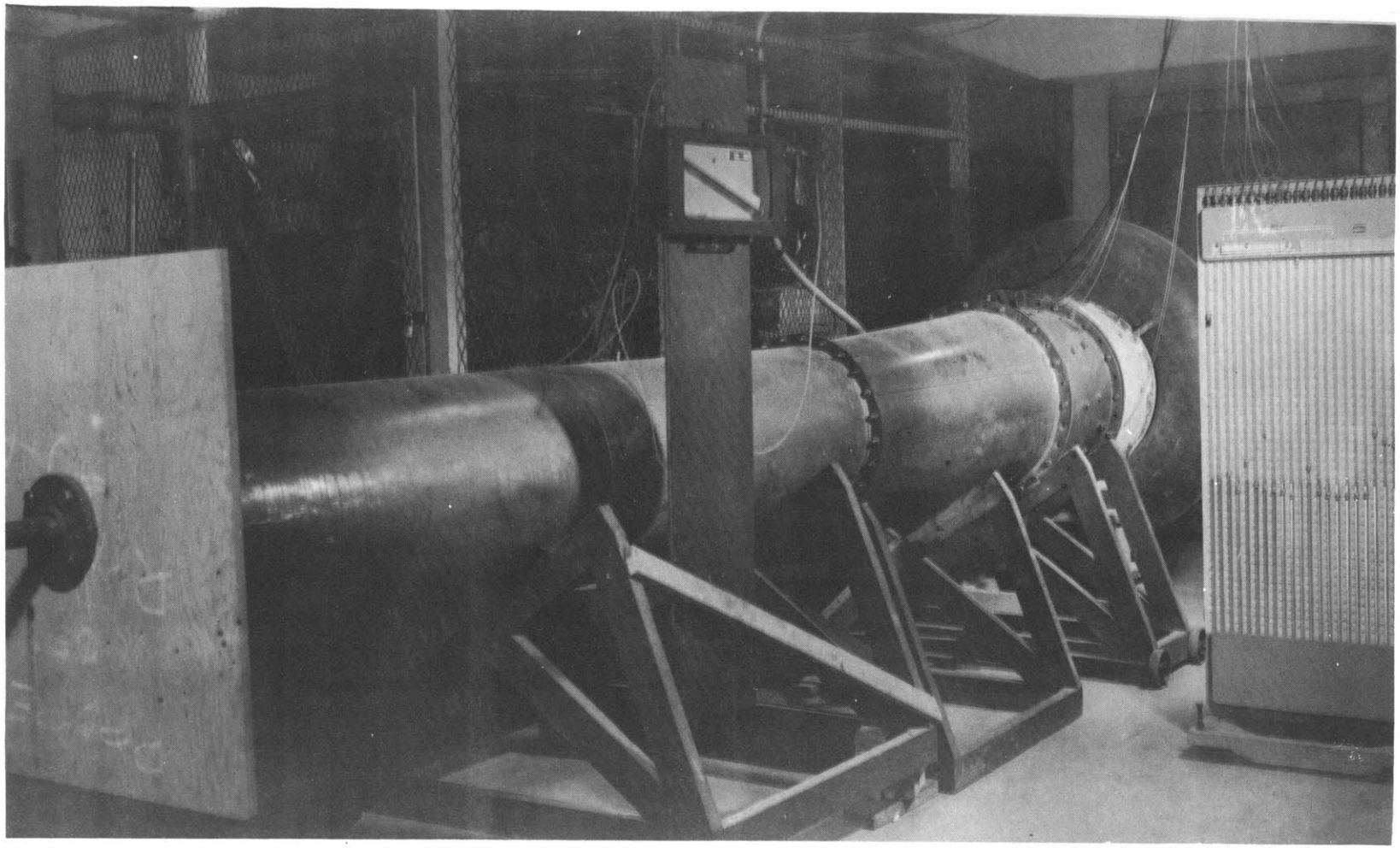

FIG. 1 TEST APPARATUS

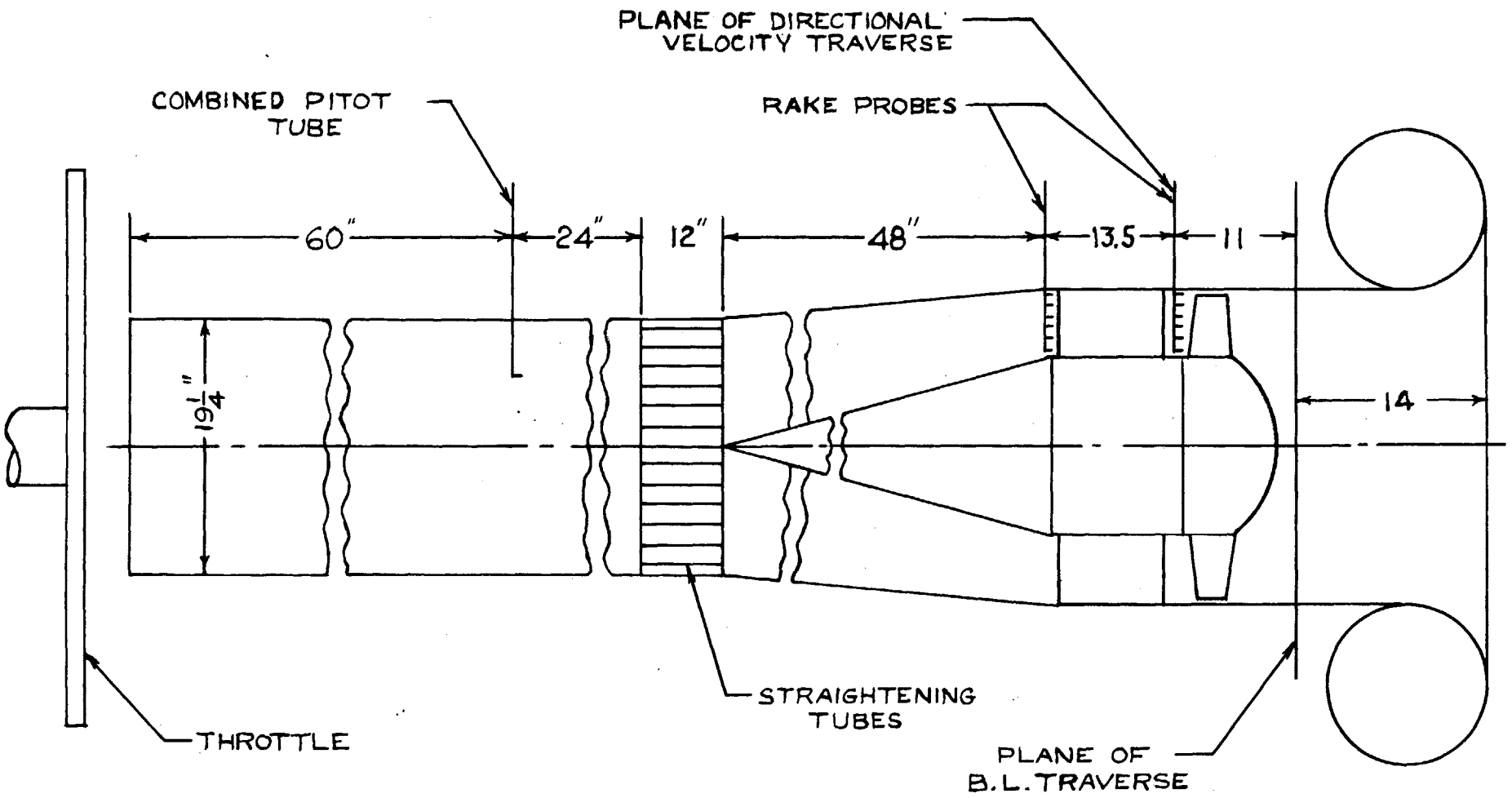

FIG. 2 - TEST SETUP

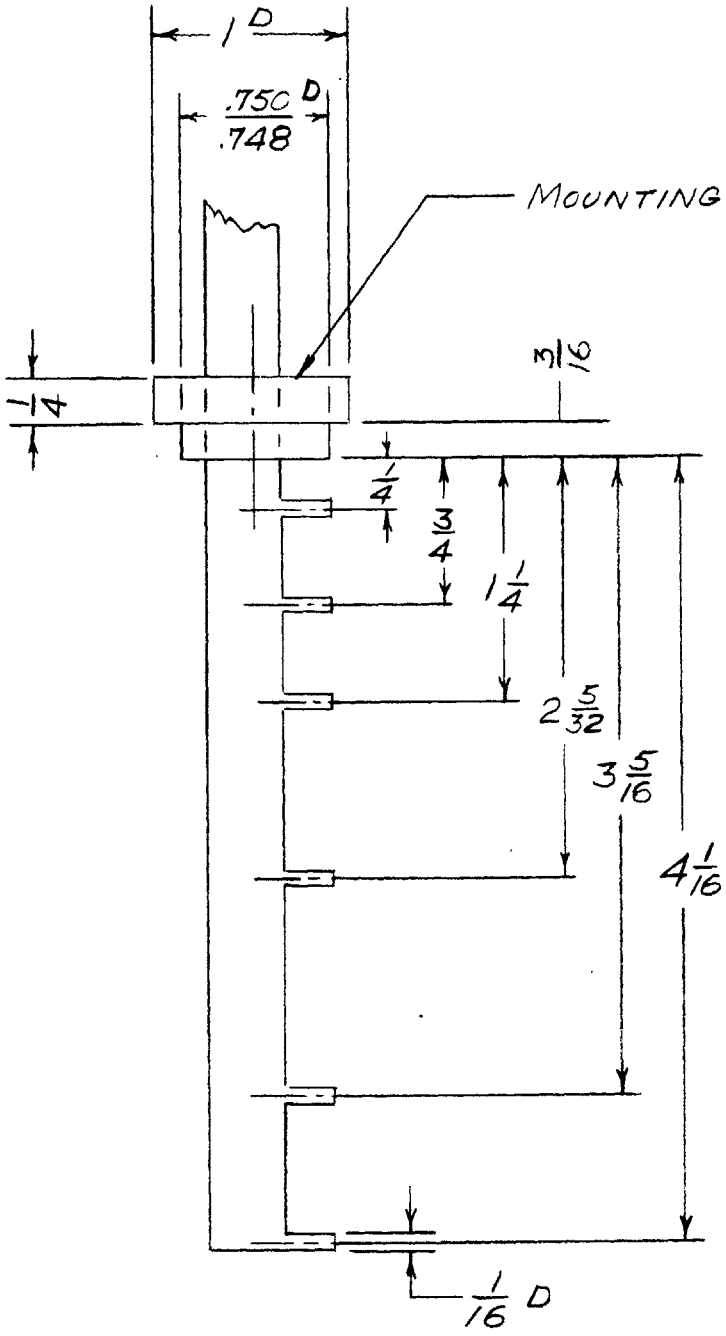

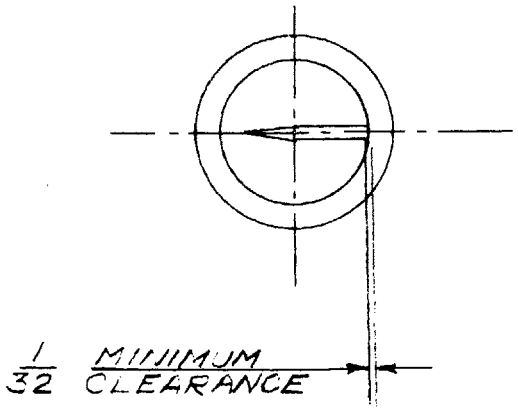

BEHIND STATOR : AS SHOWN

BEHIND ROTOR : KIEL TYPE WITH 1/8" SHROUDS

STAGNATION PRESSURE RAKES

FIG. 3

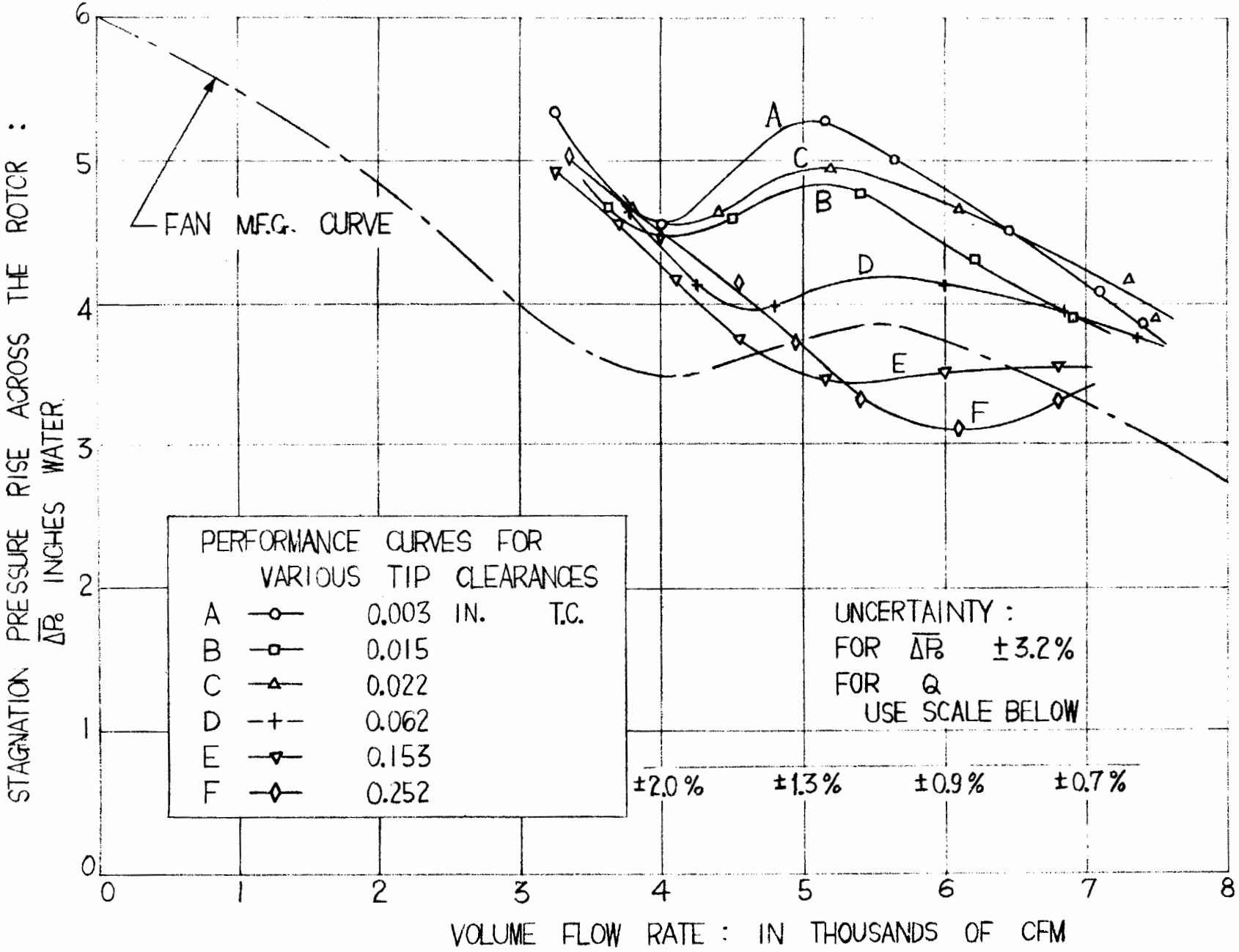
STAGNATION PRESSURE RISE ACROSS THE ROTOR : $\overline{\Delta P_o}$ INCHES WATER
VOLUME FLOW RATE : IN THOUSANDS OF CFM
FAN MF.G. CURVE
A
B
C
D
E
F
PERFORMANCE CURVES FOR VARIOUS TIP CLEARANCES
A 0.003 IN. T.C.
B 0.015
C 0.022
D 0.062
E 0.153
F 0.252
UNCERTAINTY :
FOR $\overline{\Delta P_o}$ ±3.2%
FOR Q
USE SCALE BELOW
±2.0 % ±1.3 % ±0.9 % ±0.7 %
0 1 2 3 4 5 6 7 8
0 1 2 3 4 5 6

Fig. 4

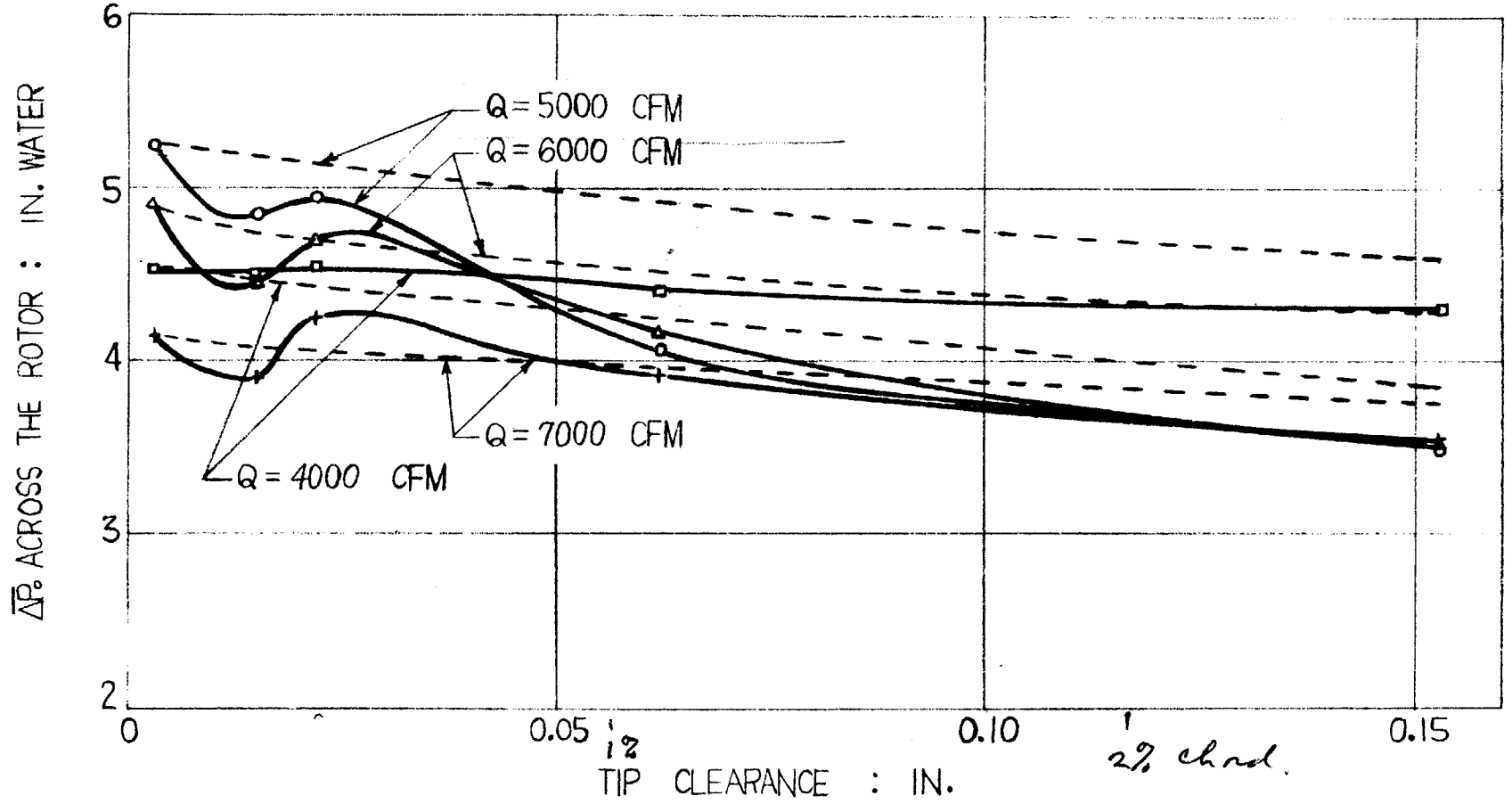

FIG. 5

DOTTED LINES ARE PREDICTED FROM THE IDEALIZED MODEL

VELOCITY PROFILES IN FRONT OF ROTOR
FOR 0.022 IN. T.C.

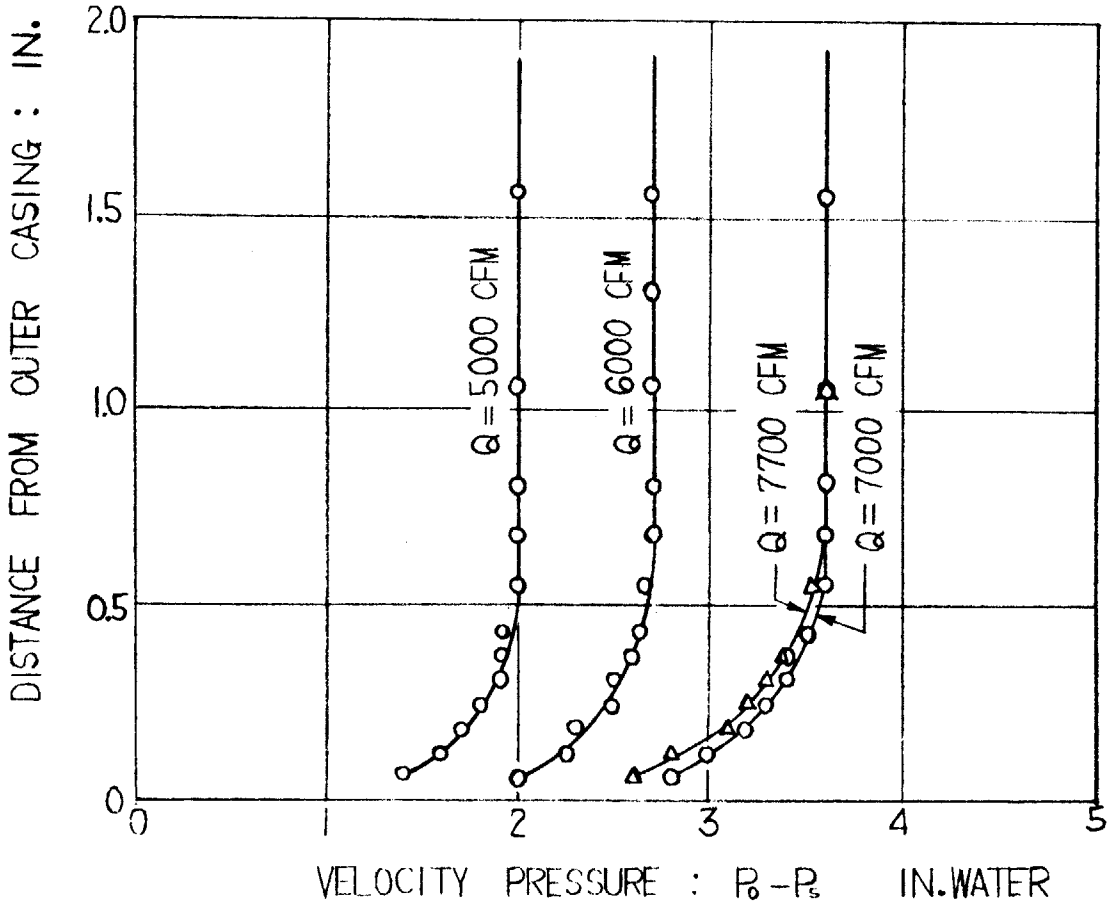

FIG. 6

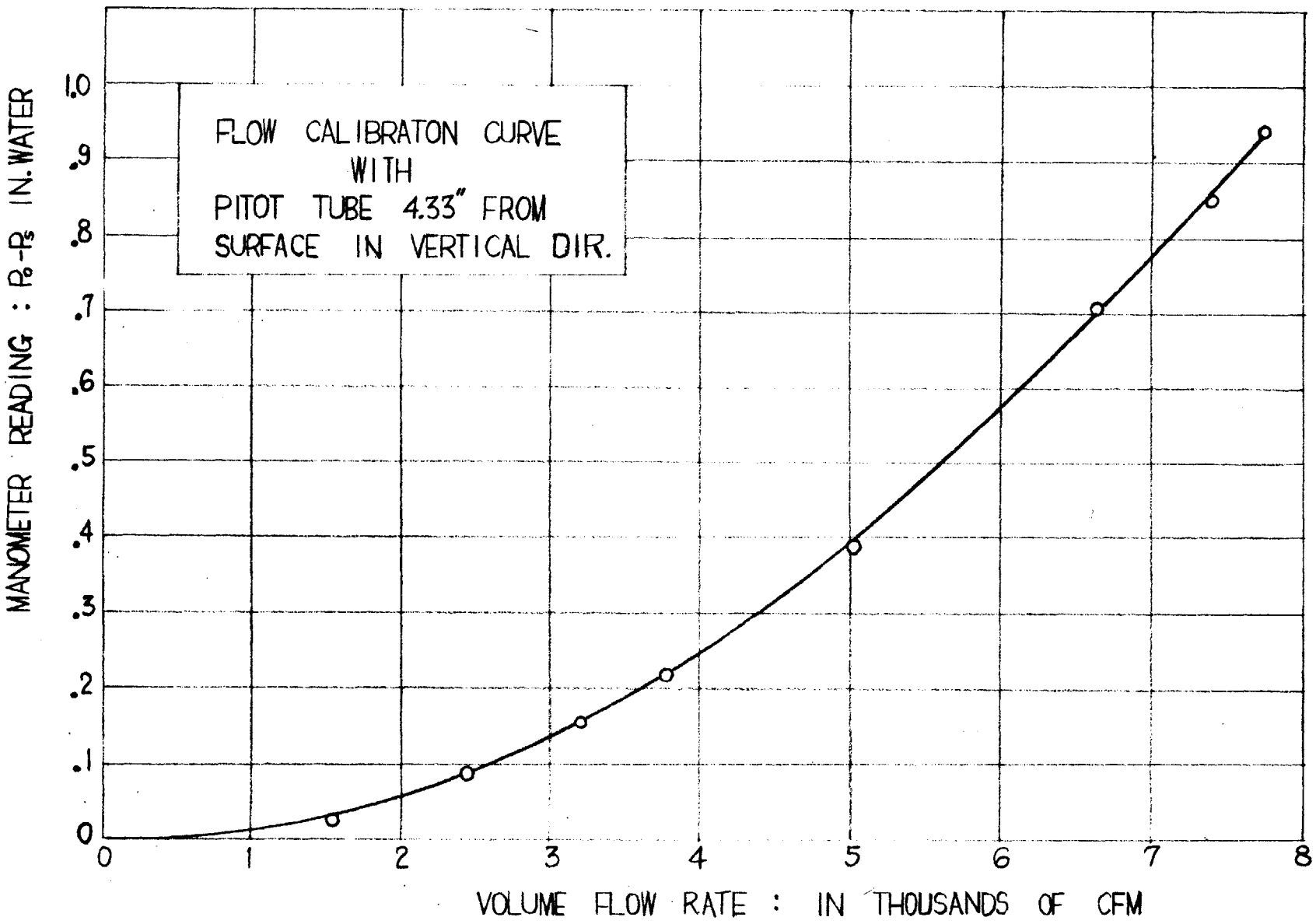
FLOW CALIBRATON CURVE
WITH
PITOT TUBE 4.33" FROM
SURFACE IN VERTICAL DIR.
MANOMETER READING : Po-Ps IN. WATER
0
.1
.2
.3
.4
.5
.6
.7
.8
.9
1.0
0
1
2
3
4
5
6
7
8
VOLUME FLOW RATE : IN THOUSANDS OF CFM

Fig. 7

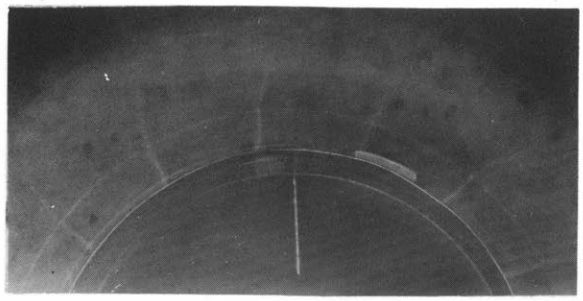

6,000 CFM

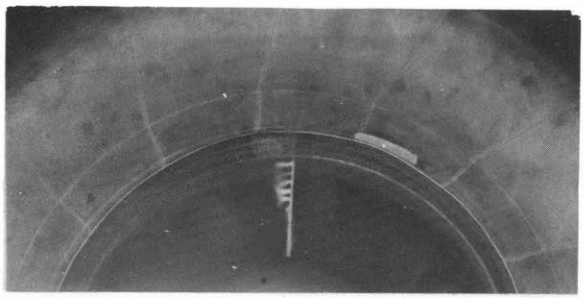

3,800 CFM

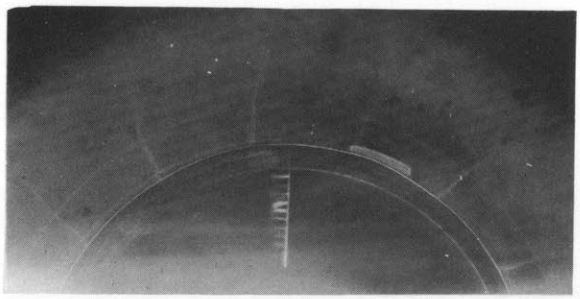

2,500 CFM

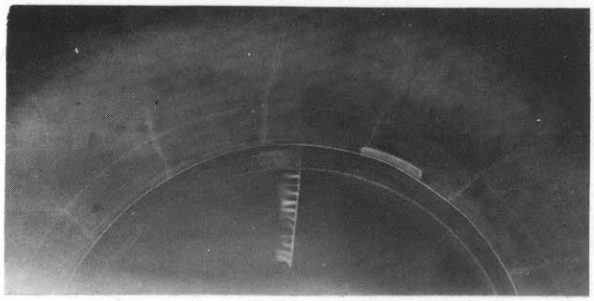

0 CFM (APPROX.)

FIG. 8 TUFTS AT ROTOR INLET

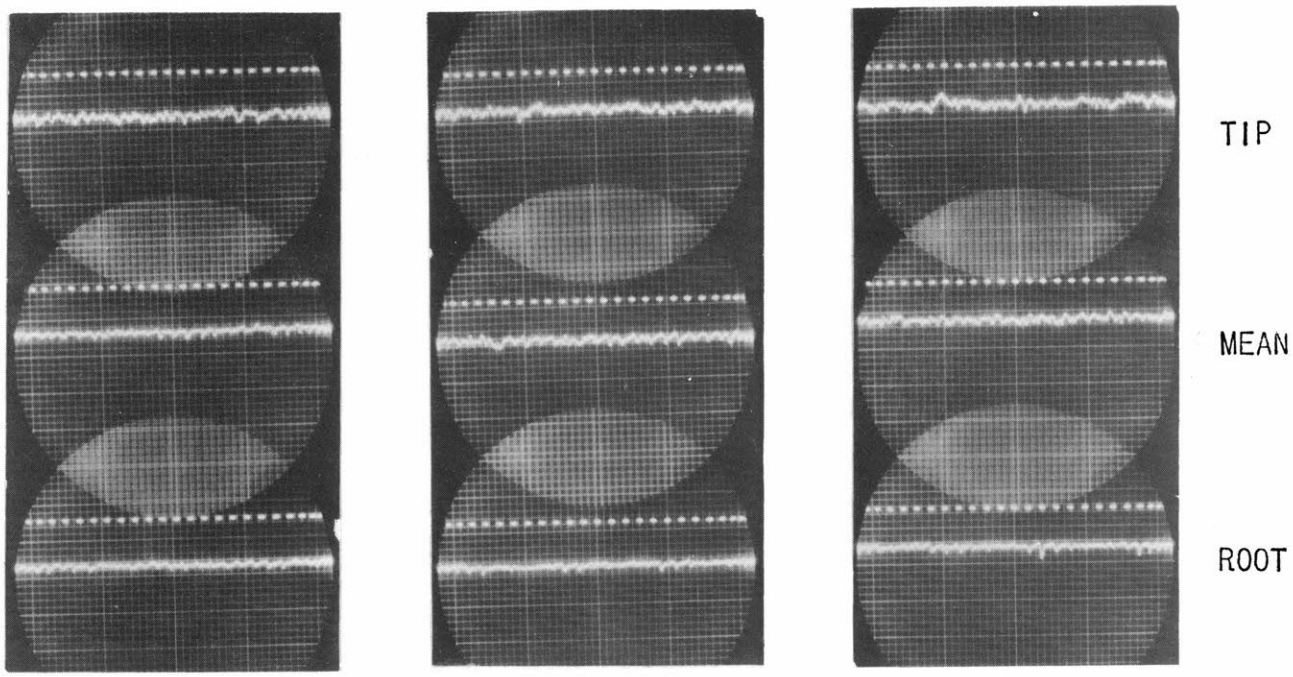

7,300 CFM 6,100 CFM 5,200 CFM

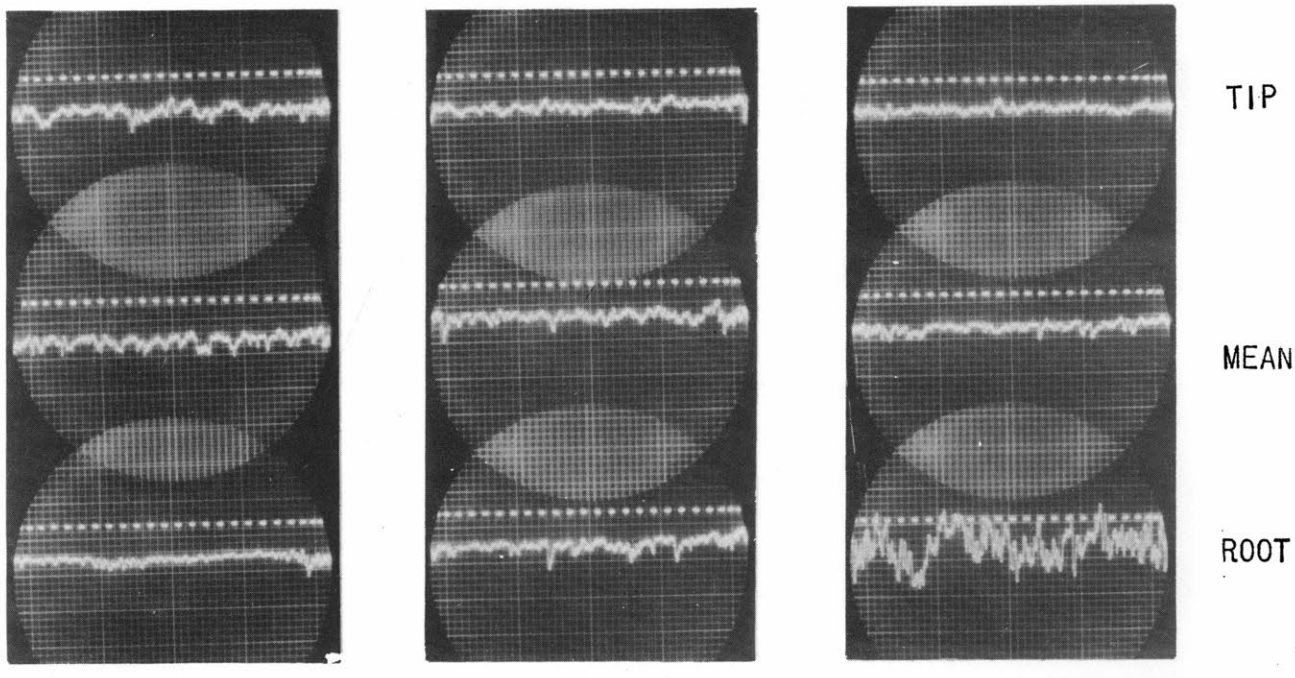

4,400 CFM 3,800 CFM 3,250 CFM

FIG. 9 OSCILLOSCOPE TRACES BEHIND ROTOR AS PICKED-UP BY HOT-WIRE ANEMOMETER PROBE (0.022 IN. TIP CLEARANCE)

FIG. 10 (a)

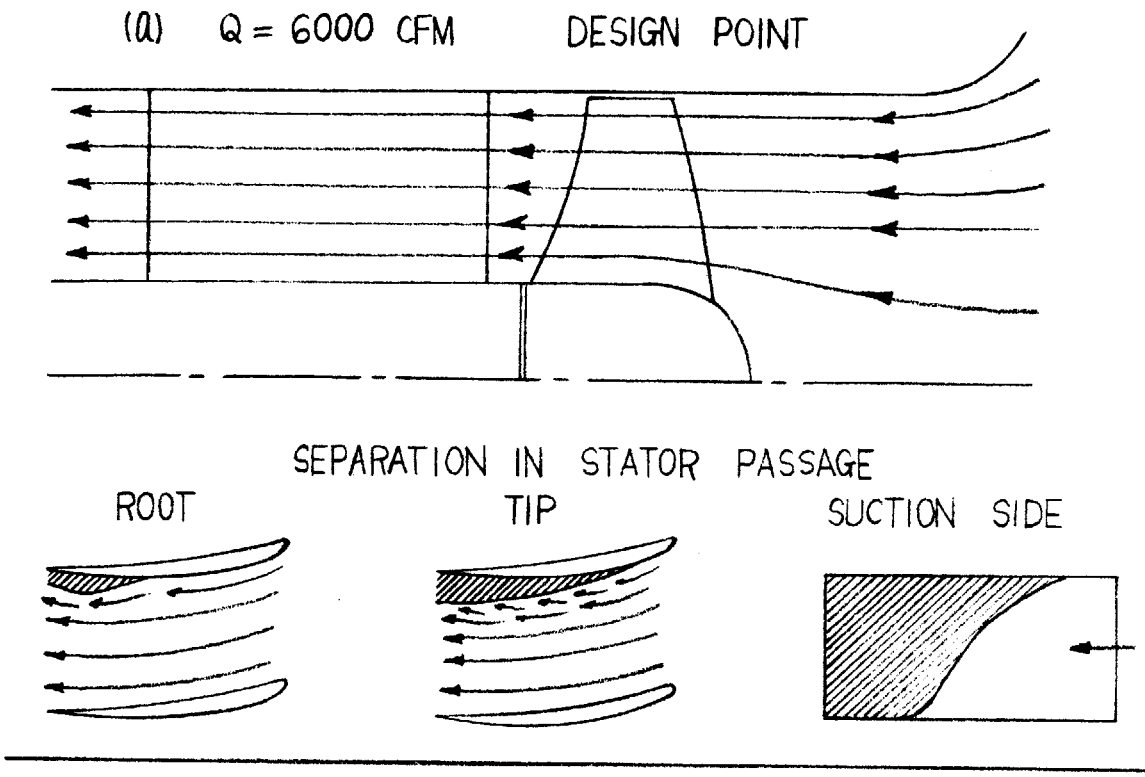

ESTIMATED FLOW PATTERN

FIG. 10(b)

⊗ = NORMAL FLOW INTO PAPER

⊙ = NORMAL FLOW OUT OF PAPER

(d) Q = 3500 CFM

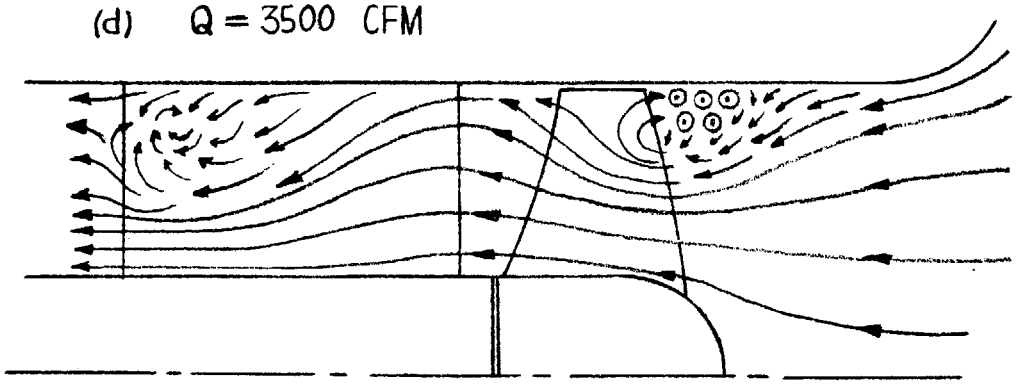

(e) Q = 3000 CFM

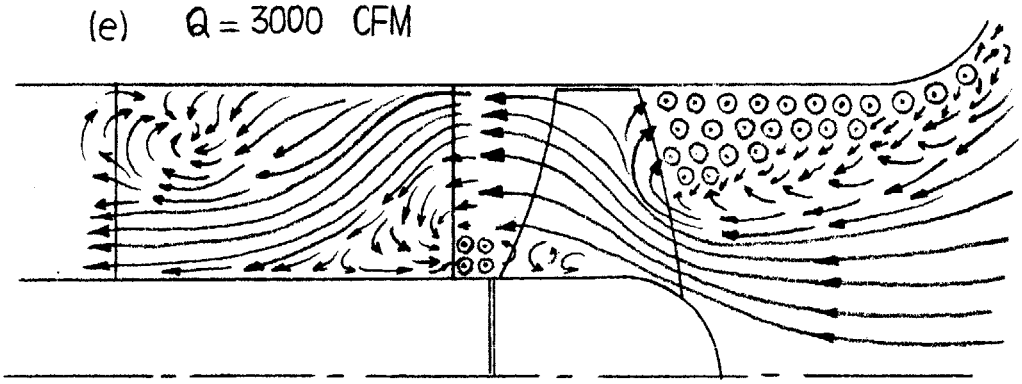

(f) Q = 2250 CFM

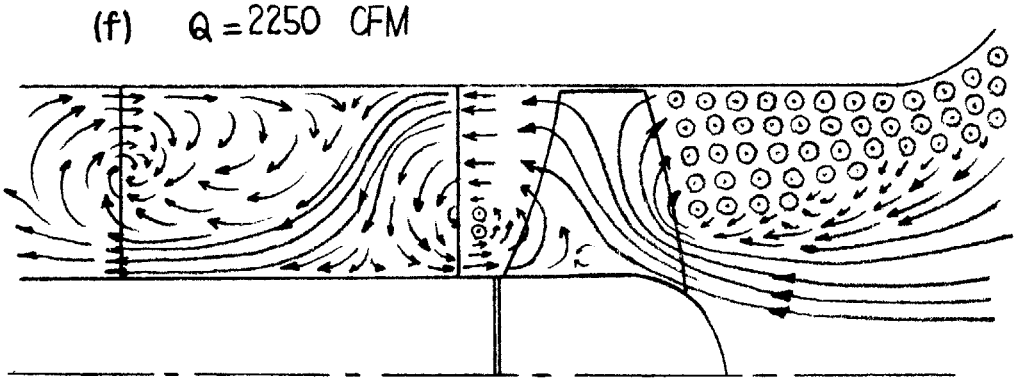

(g) Q ≒ 0 CFM

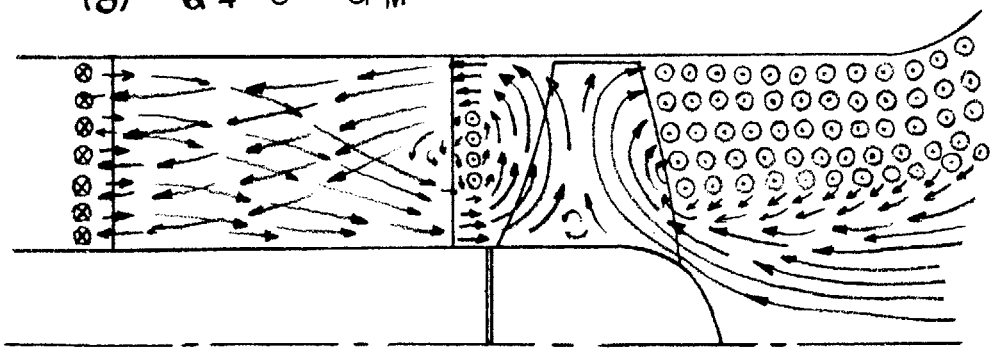

ESTIMATED FLOW PATTERN